



Studying the Structural, Optical and Electrical Properties of ZnO: SnO₂ Thin Films as an Application of a Gas Sensor Using Vacuum Thermal Evaporation Technique

^{1*}Abdulkareem Ali Hussain, ²Qahtan Nofan Abdullah

^{1,2} Department of Physics - College of Education for Pure Sciences - University of Tikrit - Tikrit - Iraq

Keywords: ZnO, SnO₂, Thermal evaporation, Thin films, Gas sensor.

ARTICLE INFO.

Article history:

-Received: 22 Oct. 2023

-Received in revised form: 02 Dec. 2023

-Accepted: 03 Dec. 2023

-Final Proofreading: 24 Dec. 2023

-Available online: 25 Dec. 2023

Corresponding Author*:

Abdulkareem Ali Hussain

AbdalKarim.a.Hussain@st.tu.edu.iq

©2023 THIS IS AN OPEN ACCESS ARTICLE
UNDER THE CC BY LICENSE
<http://creativecommons.org/licenses/by/4.0/>



ABSTRACT

In this work, thermal evaporation in vacuum technique was used to prepare the ZnO thin films as pure and doped with SnO₂ NPs on glass substrates. The XRD pattern showed the hexagonal structure of ZnO with (002) preferred orientation. The EDX technique was used to investigate the contents of the film elements prepared which consisted of Zn, Sn and O. The concentration of Zn, O and Sn in the nanostructure films was different for all doping ratios. Thickness and morphology surface of the films were calculated from cross section of the surface films (~144 nm) using scanning electron microscopy images. The FE-SEM images confirmed the ZnO nanostructures and modifications of the morphology when adding SnO₂. The pure film deposited was dense and structured; while ZnO: SnO₂ (1,5 % wt) was a nanostructure. The optical band gap and Transmittance increased with the increase in the doping ratio of SnO₂, while the absorption spectrum decreased for the prepared thin films. The prepared films showed different responses to the gas sensing at two different operating temperatures (100, 200 °C) and the doping ratio increased the sensor value of the gas at an optimum temperature of (200 °C).

دراسة الخواص التركيبية والبصرية والكهربائية لأغشية ZnO: SnO₂ الرقيقة

كتطبيق لمتحسس غازي باستخدام تقنية التبخر الحراري في الفراغ

عبد الكريم علي حسين¹، قحطان نوفان عبد الله²^{1,2} قسم الفيزياء - كلية التربية للعلوم الصرفة - جامعة تكريت - تكريت - العراق

المخلص

في هذا العمل، تم استخدام تقنية التبخر الحراري في الفراغ لتحضير أغشية ZnO النقية والمخلوطة بأوكسيد القصدير (SnO₂) على ركائز زجاجية. أظهر نمط XRD أن بنية ZnO سداسية مع اتجاه سائد (002). تم استخدام تقنية EDX لفحص محتويات العناصر للأغشية المحضرة. كان الغشاء يحتوي على Zn، Sn، O. وكان تركيز كل من Zn و O و Sn مختلفاً بالنسبة لجميع نسب التطعيم. تم حساب السمك ومورفولوجيا السطح للأغشية بتقنية المقطع العرضي وكان سمك الغشاء حوالي (144 nm) باستخدام تقنية المجهر الإلكتروني. أكدت نتائج (FE-SEM) التراكيب النانوية لأغشية ZnO واختلاف التشكيل عند إضافة الشوائب SnO₂. كان غشاء أوكسيد الخارصين النقي منتظماً كثيفاً. ومع ذلك، كان ZnO:SnO₂ بنسب تطعيم (1,5 % wt) عبارة عن تركيب نانوي. زادت فجوة الطاقة والنفذية مع زيادة نسبة التطعيم بأوكسيد القصدير SnO₂، بينما انخفض طيف الامتصاص للأغشية الرقيقة المحضرة. أظهرت الأغشية المحضرة استجابات مختلفة لاستشعار الغاز عند درجتي حرارة تحضير مختلفتين (100، 200 °C) وزادت نسبة التطعيم من قيمة حساسية الغاز عند درجة حرارة تبلغ (200 °C).
الكلمات المفتاحية: أوكسيد الخارصين، أوكسيد القصدير، التبخر الحراري في الفراغ، الأغشية الرقيقة، متحسس غازي.

1. Introduction

Due to their critical role in solving several fundamental physics issues and their prospective use as innovative materials, nanostructured semiconductors have attracted a lot of attention in recent years [1,2,3], particularly the wide-gap semiconductors with E_g values of (3.37 and 3.6 eV) at (300 K) for zinc oxide (ZnO) and tin oxide (SnO₂) [4,5]. Due to their wide range of uses, particularly as gas detectors or general reagents, several researchers have expressed interest in these molecules [6,7,8]. Since it is now a significant and independent branch of solid-state physics and deals with a thin layer of very small thickness, thin film technology is one of the most significant methods that contributed to the development and study of semiconductors. Using a variety of methods, including thermal vaporisation in vacuum, the solid is created in the form of thin layers that are placed on a solid foundation known as the substrate [9]. ZnO is a transparent conduction oxide with high infrared reflectance and high transmittance in the visible part of the spectrum [10]. Today, solid-state gas sensors are mostly utilised as operational tools to gauge the amount of toxic, dangerous, polluting, and combustible gases present in atmospheres. These metal oxide-based solid-state semiconductor gas sensors are widely employed. Due to the spectrum of conduction barriers provided by materials like zinc oxide (ZnO) and tin oxide (SnO₂), an n-type material with relatively few oxygen adsorption sites accessible is useful for sensing applications [11,12]. To improve the sensitivity, gas response, and selectivity, several additional oxides, including CdO, WO₃, ZnO, SnO₂, and CeO₂, have been investigated [13,14]. In this study, the thermal evaporation in vacuum (PVD) technique is used to create the ZnO thin films as pure and doped with SnO₂ (0, 1, and 5 % wt). The use of XRD, SEM, EDS, and the electrical characteristics I-V of the produced thin films analysis determines how composition changes of ZnO and SnO₂ affect the structural, morphological, compositional, and optical properties of films. After that, the NO₂ test gas is used to gauge how the thin film samples responded to gas sensor. The study also investigates the sample's operating temperature sensitivity, selectivity, response speed, and recovery speed.

2. Experiment

In this paper, thin films were obtained by using the vacuum thermal evaporation technique. The Edward 306 thermal evaporation system was used to prepare the ZnO thin films as pure and doped with SnO₂. They were heat-resistant in a molybdenum boat under a pressure of about (2.1×10^{-5} Tor). The substrate for the boat distance was kept at (12 cm). The thin films in this study were deposited on glass substrate made of glass strips with a thickness of (1 mm) and dimensions (26×76 mm²). After the process of cleaning the glass substrates, the Zinc powder (Zn) with a purity of (99.92) was used, mixed and milled by an agate mill with the weight ratios of tin (Sn) with a purity of (99.99) in weight ratios (1 and 5 % wt) of Sn. Finally, the films were extracted from the vacuum thermal evaporation after deposition and then placed in the furnace for thermal oxidation at a temperature of (450 °C) for two hours to obtain the zinc oxide films as pure and doped with SnO₂.

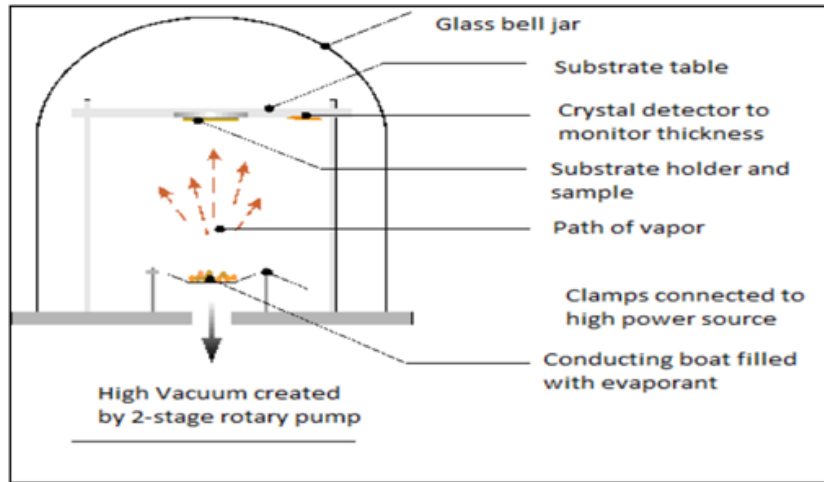


Fig. 1. the interior of the thermal vaporization chamber

3. Results and Discussion

3.1 The XRD Results

The results of the XRD scan of ZnO: SnO₂ (0, 1, and 5 % wt) thin films on the glass substrate at room temperature are shown in Fig. 2. The XRD pattern showed that the pure ZnO film and all doped films had a polycrystalline structure. The XRD ZnO pattern showed several peaks (002), (110) and (201) and the preferred orientation was (002) at 2θ (34.85°). The thin film of the ZnO was of a hexagonal structure. This is consistent with the results of [15,16]. When adding SnO₂, one peak referring to SnO₂ at 2θ of (78.15926°) at (400), the structure of SnO₂ was cubic. These results were matched with the ASTM International Material Inspection Label numbered (01-075-1526), (00-050-1429), and (00-006-0395). Peak intensity and crystal structure regularity were both improved when the doping ratio increased by (5 %). Scherer's formula was used to obtain the average crystallite size (D) [17]:

$$D = \frac{k\lambda}{\beta \cos\theta} \dots\dots\dots(1)$$

Where the wavelength XRD is (λ = 1.5406 Å), K is a constant, β is the Full Width at Half Maximum (FWHM) which equals (0.94). The size of pure ZnO crystals (15.784 nm) decreased when the doping ratio increased as (1 and 5 % wt).

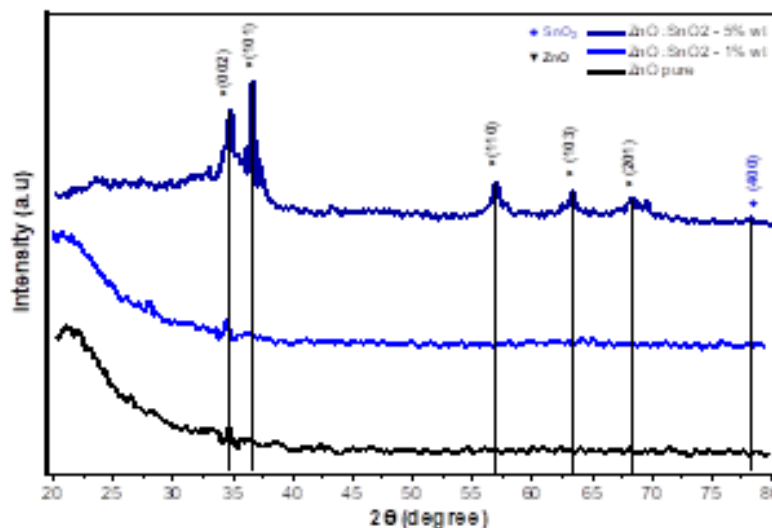


Fig. 2. the X-ray diffraction patterns of ZnO films doped with SnO₂ (0,1,5) % wt prepared by using the thermal evaporation in vacuum technique

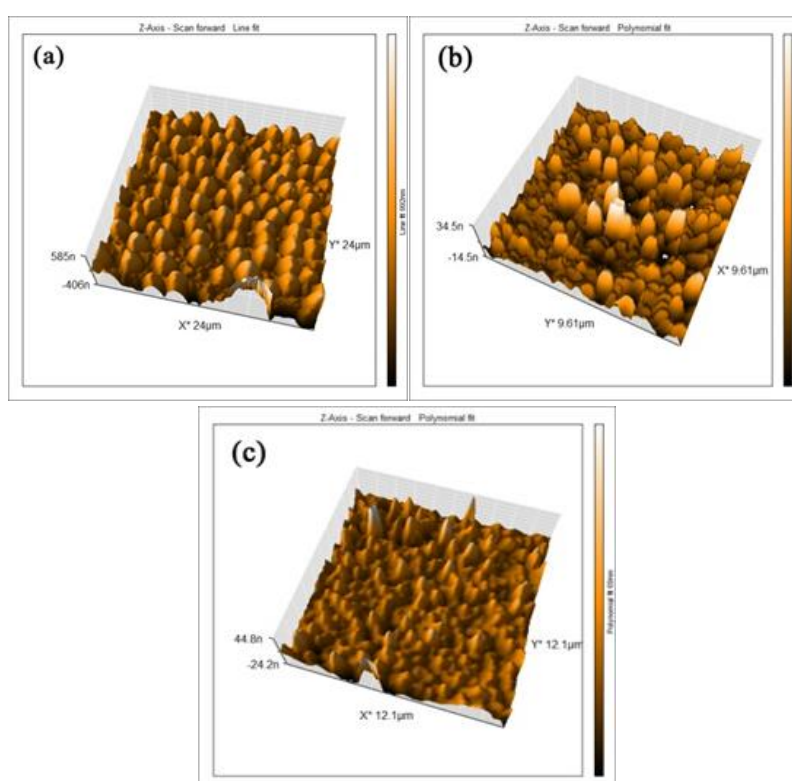
3.2 The AFM results

The AFM images of the ZnO: SnO₂ (0, 1, and 5 % wt) films prepared by using the thermal evaporation in vacuum technique at different doping ratios on glass substrate are shown in Fig. 3 (a,b,c), were measured

throughout a ($5 \mu\text{m} \times 5 \mu\text{m}$) region of the film surface. The 3D images of ZnO: SnO₂ thin films clearly showed that the grain size of the as-prepared thin films reduces with increasing the doping ratio. This result further validates the SEM findings. In comparison to the other films, ZnO: SnO₂ (1 % wt) from SnO₂ contained particles with a big size. As for the results of root mean square (RMS), the surface roughness of the ZnO: SnO₂ films was sensitive to the doping ratio. The films roughness increased with the increase in their doping ratio. In fact, the doping ratio has a clear effect on the surface topography of the prepared films [18].

Table 1. the value of the root mean square (RMS) values of surface roughness and grain size for the ZnO films pure and doped with SnO₂ (0,1,5) % wt

Sample	Roughness Average (nm)	Root Mean Square (nm)	Diameter size (nm)
Pure ZnO	701.9	128.8	112.7
1% SnO ₂	366.6	10.90	8.597
5% SnO ₂	233.6	8.440	6.351



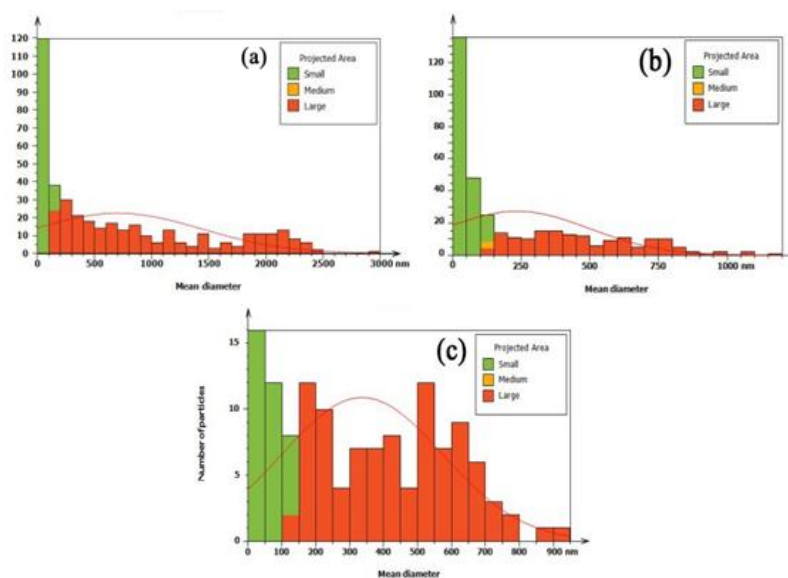
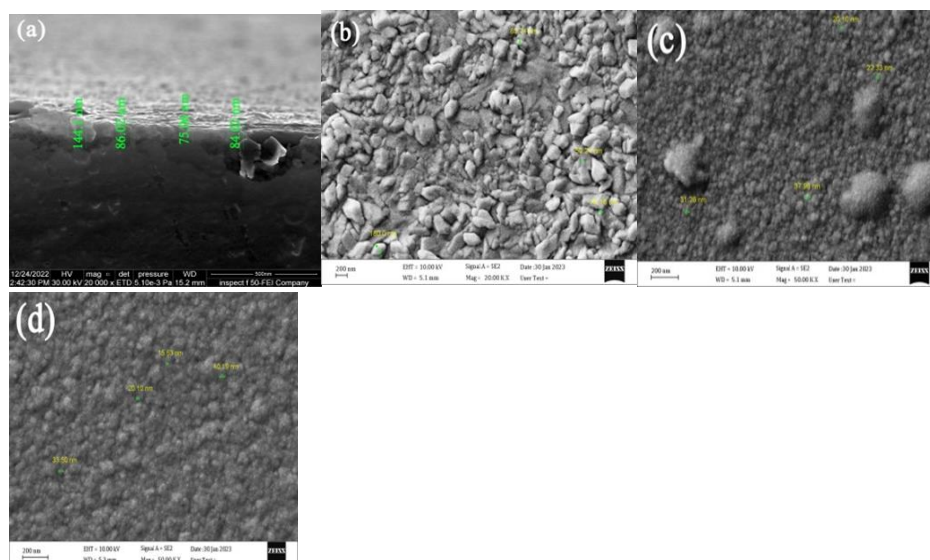


Fig. 3 (a, b, c). the three-dimensional AFM images for the ZnO films pure and doped with SnO₂ (0, 1, & 5 % wt) prepared by using the thermal evaporation in vacuum technique

3.3. The FE-SEM results

Figure (4-a) shows the SEM cross sectional views of pure ZnO film on glass substrate with a thickness of about (144 nm). Figure (4-b) shows the statistical distribution of film thickness by the cross section. Figure (4-c) shows the SEM images of ZnO thin films doped with (0, 1, & 5 % wt) of SnO₂ nanocomposite films. The SEM images of pure ZnO show dispersed agglomerated nanoparticles with stone-like shapes. However, the SEM images of ZnO: SnO₂ (1 and 5 % wt) show a porous agglomerated nanoparticle shows pure ZnO. Such morphologies are beneficial because they produce an electron-conducting channel through interconnected nanoparticles [19,20,21]. Figures 4(e, f, and g) show the ZnO thin films as pure and doped with SnO₂ (0, 1, & 5 % wt) analysed by using EDX. The EDX analysis confirmed that the thin films consisted of zinc (Zn), (Sn) and oxygen (O) only.



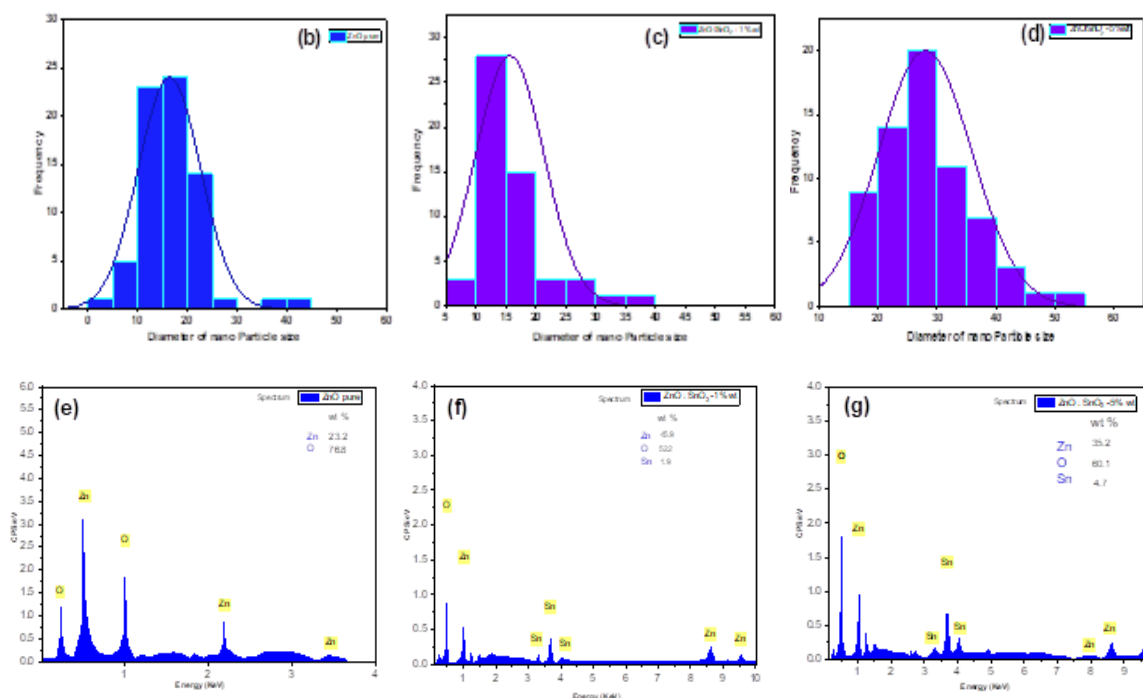


Fig. 4. (a) a cross sectional image of pure ZnO film; (b, c, and d) the FE-SEM image and statistical distribution of nanoparticles; (e, f, and g) the EDX result for the ZnO films as pure and doped with SnO₂ (0, 1, & 5 % wt) prepared by using the thermal evaporation in vacuum technique

4.3. The Optical properties results

Fig. 5(a) shows the absorbance spectrum of ZnO film as pure and doped with (1 & 5 % wt) of SnO₂. The UV–Vis spectra of ZnO thin films are shown in Fig. 5(a). It can be seen that the maximum absorbance of (494 nm) for (5 %) disappeared completely. The absorption spectrum showed an opposite behaviour to permeability due to the logarithmic relationship, as the absorbance of the films decreased by increasing the distortion with tin oxide at the two distortion ratios (1 & 5 % wt). In addition, the absorbency of all films decreased with increasing the wavelength due to the low energies of the incident photons and their inability to raise electrons from the valence band to the conduction band because of the inverse relationship between the wavelength and the photon energy [22,23]. Fig. 5(b) depicts the optical transmittance properties of the films measured using an UV–Vis spectrophotometer in the range of (300–1100 nm). All films exhibited good transmittance properties at the visible region, showing a sharp band edge at approximately (400 nm) for pure ZnO, at (392 nm) for ZnO: SnO₂ (1 % wt) and at (443 nm) for ZnO: SnO₂ (5 % wt). The transmittance increased with increasing the doping ratios. The values of optical energy gap ($E_{g_{opt}}$) for the ZnO films as pure and doped with SnO₂ deposited on glass substrate were used to find the type of optical transition by plotting the relations $(\alpha h\nu)^2$ versus photon energy ($h\nu$) (where α represents the absorption coefficient, h is the Planck constant, and ν is the frequency of photon), and selecting the optimum linear part. E_g was found for all thin films. From fig. 5(c), it can be observed that increasing the SnO₂ content from (1%) to (5 % wt) led to increasing the optical band gap from (3.261 eV) to (3.801 eV). This result is consistent with the results of previous studies [24]. Doping led to the decreased levels of localized near valence band (decreasing tails in the optical energy gap as a result of crystallinity enhancement increases the optical band gap [25].

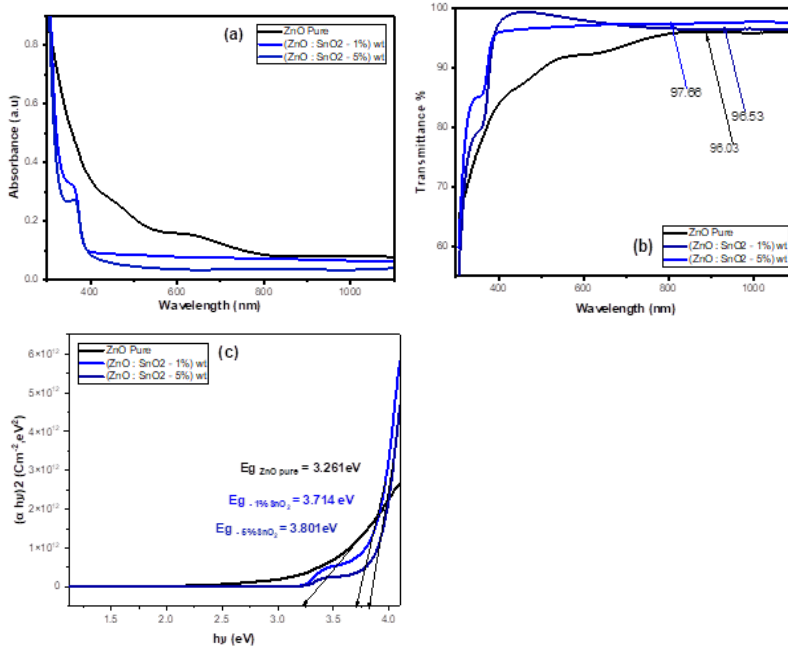


Fig. 5 (a, b, and c). the optical properties complying with the spectrum of absorption, transmittance and optical energy gap, respectively, of the ZnO films as pure and doped with SnO₂ (0, 1, & 5 % wt) prepared by using the thermal evaporation in vacuum technique

5.3. Results of electrical characteristics

The electrical properties for the ZnO films as pure and doped with SnO₂ at different ratio deposited on glass substrate include the I-V obtained from the examination of the thin films of ZnO as pure and doped with SnO₂. Figures 6(a, b, and c) show the properties of the current voltage of the ZnO films, pure and doped with SnO₂ (0, 1, & 5 % wt) deposited on the pure glass at room temperature with front and reverse bias. In this regard, the current increased with the voltages applied and the current was almost the same in biases, but the intensity of lighting (0.3 watt) on the thin film had a small effect. However, as it is clear from the figures of the sample doped with (1 %) of tin oxide that in the dark state, the current was stable and constant with increasing voltages. While the appropriate light intensity with the temperature falling with the light worked to change the current behaviour observed in the dark. This indicates that the distortion ratio improved the results of the electrical properties of the prepared material. Figures 6(a,b, and c) clarify the relationship of current with voltages that revealed the connection Ohmic between the film and the electrodes [26,27].

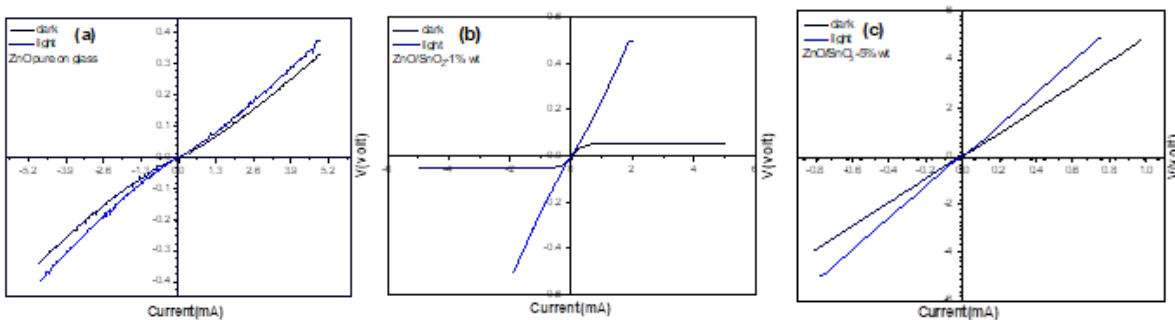


Fig. 6 (a, b, and c). the electrical properties (I-V) of the ZnO films as pure and doped with SnO₂ (0, 1, & 5 % wt) prepared by using the thermal evaporation in vacuum technique

6.3. The Gas sensing results

The majority of simple metal oxide sensors struggle with a long-range instability and sensitivity-cross junction. In order to overcome these subjective or innate challenges, the chemical composition of the sensitized layer is adjusted by doping. Moreover, the effective surface dopants enhance the sensor performance. To investigate and compare the gas sensing properties of ZnO: SnO₂ thin films (0, 1, & 5 wt %), the sensors were tested at different temperatures of (100 and 200 °C). Responses were measured with NO₂. As shown in Fig.7(a, b, c, d, e, and f), temperature had a clear effect on the response of the NO₂ gas sensor. Through the passage of time, the resistance to the membrane-based sensor structure of pure ZnO films was varied at an operating temperature of (100 °C) with about (86 %) sensing for NO₂ gas. When introducing the target gas (NO₂) into the chamber, the

film resistance increased due to the oxidizing behaviour of the NO₂ gas. The sensing value of the gas decreased to (55 %) when the operating temperature increased to (200 °C). When adding (5 %) of SnO₂, the thin film showed a good response at a temperature of (100 °C), and the gas sensing response was (64.7 %) compared to the rest of the previous films. But with high temperatures, this percentage of the films showed an increase in the response rate until it reached (88.6 %) at a temperature of (200 °C). The reason is mostly because the crystal structure in these films was regular and intertwined, as explained by the results of XRD as being the most regular than other films [28,29].

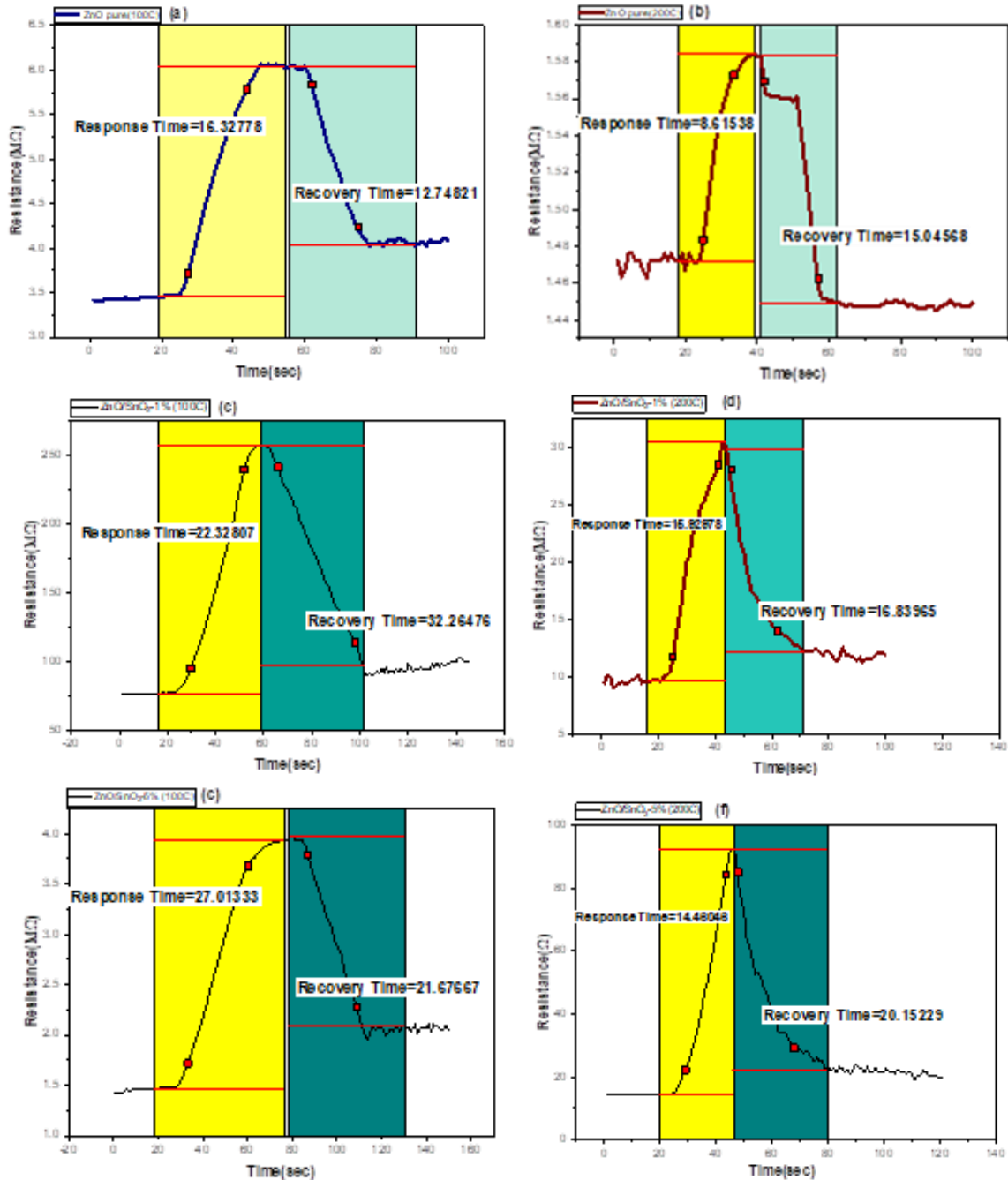


Fig. 7 (a, b, c, d, e, and f). the response and recovery time at two operating temperatures of (100 and 200 °C) for the ZnO thin films as pure and doped with SnO₂ (0, 1, & 5 % wt) deposited by using the thermal evaporation in vacuum technique

7. Conclusions

This work demonstrated the use of thermal evaporation method in synthesizing the ZnO: SnO₂ (0, 1, & 5 % wt) films nanostructures for gas sensing applications. The performance of the various nanostructures for gas sensing was examined and compared using the ZnO: SnO₂ films. Comparative gas sensing experiments revealed that the

ZnO: SnO₂ films performed better than other materials, which might be ascribed to the materials' high porosity, increased number of active sites, and incorporation of core-outer junctions. The ZnO: SnO₂ nanostructures created thus far have a lot of potential for use in gas sensor applications. Additionally, the synthesis of additional nanostructures based on metal oxide materials, such as: ZnO: CdO, ZnO: In₂O₃, ZnO: WO₃, and ZnO: TiO₂, may be accomplished using the method provided by this study.

References

- [1] Tricoli, A.; Righettoni, M. & Teleki, A. (2010). Semiconductor gas sensors: dry synthesis and application. *Angewandte Chemie International Edition*, 49(42):7632–7659.
- [2] Miller, D.R.; Akbar, S.A. & Morris, P.A. (2014). Nanoscale metal oxide-based heterojunctions for gas sensing: A review. *Sensors and Actuators B: Chemical*, 204:250–272.
- [3] Sze, S.M.; Li, Y. & Ng, K.K. (2021). *Physics of semiconductor devices*. 3rd ed. John Wiley & sons.
- [4] Wang, H. & Rogach, A.L. (2014). Hierarchical SnO₂ nanostructures: recent advances in design, synthesis, and applications. *Chemistry of Materials*, 26(1):123–133.
- [5] Özgür, Ü.; Alivov, Y.I.; Liu, C.; Teke, A.; Reshchikov, M.A.; Doğan, S.; Avrutin, V.; Cho, S.J. & Morkoç, A.H. (2005). A comprehensive review of ZnO materials and devices. *Journal of applied physics*, 98(4): 041301(1–95).
- [6] Catto, A.C.; Da Silva, L.F.; Ribeiro, C.; Bernardini, S.; Aguir, K.; Longo, E. & Mastelaro, V.R. (2015). An easy method of preparing ozone gas sensors based on ZnO nanorods. *Rsc advances*, 5(25):19528–19533.
- [7] Fan, S.W.; Srivastava, A.K. & Dravid, V.P. (2009). UV-activated room-temperature gassensing mechanism of polycrystalline ZnO. *Appl. Phys. Lett.* 95(14):142106–142106.
- [8] Korotcenkov, G. & Cho, B.K. (2012). Ozone measuring: What can limit application of SnO₂-based conductometric gas sensors? *Sensors and Actuators B: Chemical*, 161(1):28–44.
- [9] O'Hanlon, F. (2003). *A User's Guide to Vacuum Technology*. John Wiley & Sons, Inc.
- [10] Bouderbala, M.; Hamzaoui, S.; Amrani, B.; Reshak, A.H.; Adnane, M.; Sahraoui, T. & Zerdali, M. (2008). Thickness dependence of structural, electrical and optical behaviour of undoped ZnO thin films. *Physica B: Condensed Matter*, 403(18):3326–3330.
- [11] Yan, S.H.; Ma, S.Y.; Li, W.Q.; Xu, X.L.; Cheng, L.; Song, H.S. & Liang, X.Y. (2015). Synthesis of SnO₂-ZnO heterostructured nanofibers for enhanced ethanol gas-sensing performance. *Sensors and actuators B: chemical*, 221:88–95.
- [12] Yamazoe, N. (2005). Toward innovations of gas sensor technology. *Sensors and Actuators B: Chemical*, 108(1-2):2–14.
- [13] Rajput, J.K.; Pathak, T.K.; Kumar, V.; Swart, H.C. & Purohit, L.P. (2018). Tailoring and optimization of optical properties of CdO thin films for gas sensing applications. *Physica B: Condensed Matter*, 535:314–318.
- [14] Patil, D.; Patil, V. & Patil, P. (2011). Highly sensitive and selective LPG sensor based on α -Fe₂O₃ nanorods. *Sensors and Actuators B: Chemical*, 152(2):299–306.
- [15] Dahham, A.R.; Mohammed, S.J. & Mohammed, W.M. (2019). Study of the optical and structural properties of the (ZnO) membrane, which is prepared by the method of thermal steaming by using the closed oven. *Tikrit Journal of Pure Science*, 24(2):56–62.
- [16] Abdallah, B.; Kakhia, M.; Zetoun, W. & Alkafri, N. (2021). PbS doped ZnO nanowires films synthesis by thermal evaporation method: Morphological, structural and optical properties. *Microelectronics Journal*, 111:105045.
- [17] Ibrahim, A.M.E.; Isma'el, R.A.; Ibrahim, E.S. & Ibrahim, E.M. (2017). Study the structural and Optical properties of ZnO thin film. *Tikrit Journal of Pure Science*, 22(1):148–155.
- [18] Martínez, D.T.; Pérez, R.C.; Delgado, G.T. & Ángel, O.Z. (2012). Structural, morphological, optical and photocatalytic characterization of ZnO-SnO₂ thin films prepared by the sol-gel technique. *Journal of Photochemistry and Photobiology A: Chemistry*, 235:49–55.
- [19] Pakhare, K.S.; Sargar, B.M.; Potdar, S.S.; Patil, U.M. & Mane, R.D. (2022). SILAR synthesis of SnO₂-ZnO nanocomposite sensor for selective ethanol gas. *Bulletin of Materials Science*, 45(2):68(11 pages).

- [20] Zarei, S.; Hasheminasari, M.; Masoudpanah, S.M. & Javadpour, J. (2022). Photocatalytic properties of ZnO/SnO₂ nanocomposite films: role of morphology. *Journal of Materials Research and Technology*, 17:2305–2312.
- [21] Mu, S.; Wu, D.; Qi, S. & Wu, Z. (2011). Preparation of polyimide/zinc oxide nanocomposite films via an ion-exchange technique and their photoluminescence properties. *Journal of Nanomaterials*, 2011:1–10.
- [22] Islam, M.R. & Podder, J. (2009). Optical properties of ZnO nano fiber thin films grown by spray pyrolysis of zinc acetate precursor. *Crystal Research and Technology: Journal of Experimental and Industrial Crystallography*, 44(3):286–292.
- [23] Rashad, M.M.; Ismail, A.A.; Osama, I.; Ibrahim, I.A. & Kandil, A.H.T. (2014). Photocatalytic decomposition of dyes using ZnO doped SnO₂ nanoparticles prepared by solvothermal method. *Arabian Journal of Chemistry*, 7(1):71–77.
- [24] Aadim, K.A. & Essa, M.A. (2019). Structural and Optical properties of SnO₂ doped ZnO thin films prepared by Pulsed Nd: YAG Laser Deposition. *Journal of College of Education*, 3(3):109–122.
- [25] Sayadi, M.H.; Ghollasimood, S.; Ahmadpour, N. & Homaeigozar, S. (2022). Biosynthesis of the ZnO/SnO₂ nanoparticles and characterization of their photocatalytic potential for removal of organic water pollutants. *Journal of photochemistry and photobiology A: chemistry*, 425:113662.
- [26] Ibrahim, A.M.E.; Isma'el, R.A.; Ibrahim, E.S. & Ibrahim, E.M. (٢٠١٦). Study the electrical properties of ZnO/p-Si heterojunction prepared by chemical spray pyrolysis. *Tikrit Journal of Pure Science*, 21(7):162–166.
- [27] McLachlan, D.S. & Sauti, G. (2007). The AC and DC conductivity of nanocomposites. *Journal of Nanomaterials*, Volume 2007: Article ID 30389(9 pages).
- [28] Oh, E.; Choi, H.Y.; Jung, S.H.; Cho, S.; Kim, J.C.; Lee, K.H.; Kang, S.W.; Kim, J.; Yun, J.Y. & Jeong, S.H. (2009). High-performance NO₂ gas sensor based on ZnO nanorod grown by ultrasonic irradiation. *Sensors and Actuators B: Chemical*, 141(1):239–243.
- [29] Singh, A.; Sikarwar, S. & Yadav, B.C. (2021). Design and fabrication of quick responsive and highly sensitive LPG sensor using ZnO/SnO₂ heterostructured film. *Materials Research Express*, 8(4):045013.